ACS Macro Letters

Letter

pubs.acs.org/macroletters

Dispersity under Scrutiny: Phase Behavior Differences between Disperse and Discrete Low Molecular Weight Block Co-Oligomers

Bas van Genabeek, Bas F. M. de Waal, Bianca Ligt, Anja R. A. Palmans,* and E. W. Meijer*

Institute for Complex Molecular Systems and Laboratory of Macromolecular and Organic Chemistry, Eindhoven University of Technology, P.O. Box 513, 5600 MB Eindhoven, The Netherlands

Supporting Information

ABSTRACT: An experimental study is presented in which we compare the bulk phase behavior of discrete and (partially) disperse diblock co-oligomers (BCOs) with high χ–low N. To this end, oligomers of dimethylsiloxane (*o*DMS) and lactic acid (*o*LA) were synthesized, each having either a discrete number of repeat units or a variable block length. Ligation of the blocks resulted in *o*DMS–*o*LA BCOs with dispersities ranging from <1.00001 to 1.09, as revealed by mass spectroscopy and size exclusion chromatography. The phase behavior of all BCOs was investigated by differential scanning calorimetry and small-angle X-ray scattering. Compared to the well-organized lamellae formed by discrete *o*DMS–*o*LA, we observe that an increase in the dispersity of these BCOs results in (1) an increase of the *stability* of the microphase-segregated state, (2) a decrease of the overall *degree of ordering*, and (3) an increase of the *domain spacing*.

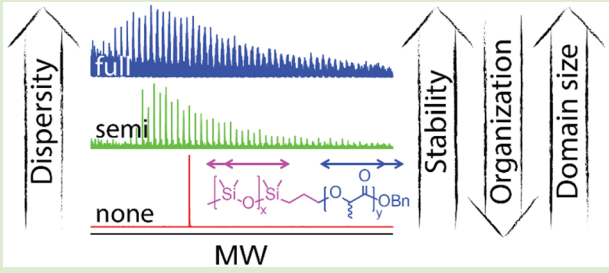

Block copolymers (BCPs) represent an important class of self-organizing materials and have been studied for many decades. By far the largest subgroup herein is the diblock copolymers, which comprise two chemically distinct polymeric entities, covalently linked to generate a linear macromolecule. The microphase separation between these polymer blocks is well understood—both theoretically and experimentally—and enables chemists to control morphologies as well as feature sizes, mainly by fine-tuning three parameters: the Flory–Huggins interaction parameter, χ; the average overall degree of polymerization, N; and the volumetric ratio of the two blocks, expressed as the volume fraction of block A (f_A) or block B ($f_B = 1 - f_A$).[1]

The increasing attractiveness of BCPs for emerging fields such as nanopatterning and nanofiltration initiated a desire to decrease the feature sizes and increase the long-range order of the formed morphologies. This has resulted in a plethora of publications describing the behavior of materials containing two highly incompatible blocks, close to or at the border of (micro)phase separation.[2] In a number of cases, these so-called "high χ–low N" block copolymers commonly share the use of one silicon-rich block (resulting in both high χ values and a high etching contrast), in combination with very short block lengths (low N).[3−8] Although it is rarely specifically addressed,[2] this trend inevitably results in a higher sensitivity of the material toward absolute changes in the (average) degree of polymerization. A simple calculation shows that elongation of the A block of an A_{15}–B_{15}-type BCP (i.e., a BCP comprising 2 blocks of 15 A-monomers and 15 B-monomers) by only a single A-monomer already results in an ∼3.3% increase in both N and f_A, which consequently may lead to complete alteration of the phase behavior. Inevitably, this also raises the question how the phase behavior is affected by the chain length and composition dispersity, both of which result in *chain-to-chain* variations in N and f_A around the average values. Of particular consideration is the fact that even low disperse polymers comprise polymer chains differing up to tens of repeat units.

As was nicely summarized by Hillmyer et al.,[9] most of the early theoretical work that employs the self-consistent field theory (SCFT) or random phase approximation (RPA) theory to address the effect of dispersity on BCP phase behavior predicts that increased dispersity will lead to an increase of the segregation strength (decrease of χN_{ODT}) over the full f_A range, as well as an increase of the domain spacing (d^*). More recently, Monte Carlo studies were performed by Matsen et al. for a BCP system that better resembles experimentally accessible low N BCPs, avoiding the approximations needed for SCFT and RPA calculations.[10,11] The BCPs evaluated in this work were only disperse in one of the two blocks. The computational results confirmed the elaborate experimental work by Hillmyer and co-workers on relatively low MW poly(ethylene-*alt*-propylene)-*b*-polylactide (PEP–PLA) and poly(styrene-*b*-isoprene) (PS–PI).[12−14] Careful analysis of their phase behavior revealed that all BCPs formed microphase-segregated structures, in which an increased dispersity resulted in an increase of the segregation strength,[12] as well as an increase of the domain spacing for polymers with similar average length and composition.[13] Interestingly, the uniformity of the structures seemed "independent of the size distribution

Received: April 9, 2017
Accepted: June 8, 2017
Published: June 14, 2017

DOI: 10.1021/acsmacrolett.7b00266
ACS Macro Lett. 2017, 6, 674–678

of the polymers that comprise it".[14] Still, with an overall dispersity range of $1.1 < Đ < 1.4$, a large portion of the low-dispersity playground remains uncovered. Moreover, beautiful work of Chang and co-workers[15−17] revealed that HPLC fractionation of various samples of "monodisperse" PS-*b*-PI ($\bar{M}_n$ > 20 kDa, $Đ \approx 1.02$) resulted in better organized phases than those present in the parent material. This not only highlights the vast number of different polymeric species present in polymer samples that are often misleadingly labeled "monodisperse" but also restates the question: how perfect do we have to define our molecules to attain the desired (self-assembly) properties?[18]

Recently, we reported on the self-assembly of "truly monodisperse" or discrete (i.e., $Đ < 1.00001$) diblock co-oligomers (BCOs), composed of oligodimethylsiloxane (*o*DMS) and atactic oligolactic acid (*o*LA).[19] Microphase separation of the BCOs into various ordered structures was observed even for $N < 50$, despite the fact that the materials employed in this work are located in the weak phase-segregation regime because of their low molecular weights. In contrast, an analogous, disperse *o*DMS−*o*LA reference material ($Đ = 1.15$) with similar $\bar{M}_n$ and *o*LA volume fraction (f_{LA})—but slightly different end groups and interblock connectivity—did not yield ordered structures.

Surprised by this result, which is in contradiction to the work of Hillmyer et al.,[12−14] Mahanthappa et al.,[20−22] Matsushita et al.,[23,24] and numerous theoretical models,[9−11] we were encouraged to perform a more systematic study of discrete versus disperse blocks in low MW BCOs. The work presented here is accompanied by a complementary study by Hawker and co-workers on (semi)discrete/disperse BCOs.[25] Utilizing our knowledge on the *o*DMS−*o*LA system, we envisioned a set of co-oligomers with almost identical end groups and interblock connectivity but embodying four different types of dispersity: (1) discrete *o*DMS + discrete *o*LA; (2) disperse *o*DMS + discrete *o*LA; (3) discrete *o*DMS + disperse *o*LA; (4) disperse *o*DMS + disperse *o*LA. Both for practical reasons (commercial availability of the starting materials) and to minimize the risk of encountering undesired morphology changes upon changing the dispersity, we aimed for a symmetric BCO ($f_{LA} \approx 0.5$) with (average) block lengths of 15 siloxane and 17 lactic acid repeat units.

First, *o*DMS with a free carboxylic acid residue and atactic *o*LA with a free hydroxyl group were synthesized (both discrete and disperse variants), followed by straightforward ligation via carbodiimide-facilitated esterification (Scheme 1). In this way, the dispersity in each of the two blocks can be tuned independently. The synthesis of discrete *o*DMS $\mathbf{Si_{15}}$, *o*LA $\mathbf{LA_{16}}$, and subsequent coupling has been fully documented.[19] The disperse *o*DMS block $\mathbf{Si_{\sim 15}}$ was prepared in a similar way as the discrete analogue, starting from commercially available *o*DMS hydride (DP ≈ 15; $M_n \approx 1150$ Da) (Scheme S1). Disperse *o*LA $\mathbf{LA_{\sim 16}}$-**PC** was synthesized with an uncontrolled condensation reaction of lactic acid dimer, which was initially obtained via ring opening of DL-lactide (a 1-to-1 mixture of L- and D-lactide) with water (Scheme S2). A subsequent, carbodiimide-mediated polycondensation (PC) reaction of this compound with the appropriate amount of benzyl alcohol as a chain stopper resulted in the desired $\mathbf{LA_{\sim 16}}$-**PC** block. For comparison, we also prepared the disperse *o*LA block by a more commonly employed ring-opening polymerization (ROP) of DL-lactide with benzyl alcohol, in the presence of catalytic amounts of 1,8-diazabicyclo[5.4.0]undec-7-ene (DBU) (Scheme S3).

Finally, coupling of the two *o*DMS and three *o*LA blocks resulted in 6 BCOs: [$\mathbf{Si_{15}}$-$\mathbf{LA_{17}}$], [$\mathbf{Si_{\sim 15}}$-$\mathbf{LA_{17}}$], [$\mathbf{Si_{15}}$-$\mathbf{LA_{\sim 17}}$]-**PC**, [$\mathbf{Si_{\sim 15}}$-$\mathbf{LA_{\sim 17}}$]-**PC**, [$\mathbf{Si_{15}}$-$\mathbf{LA_{\sim 17}}$]-**ROP**, and [$\mathbf{Si_{\sim 15}}$-$\mathbf{LA_{\sim 17}}$]-**ROP**. The disperse blocks are indicated with a tilde (∼) character preceding the (desired) average block lengths and the methods used for the synthesis of the *o*LA blocks are abbreviated as **PC** and **ROP** for polycondensation and ring-opening polymerization, respectively. Full experimental details can be found in the Supporting Information.

All materials were purified by automated column chromatography and fully analyzed with ^{1}H NMR, ^{13}C NMR, matrix-assisted laser desorption/ionization time-of-flight (MALDI-TOF) mass spectrometry, and size exclusion chromatography (SEC) (Figures S1−S8). As depicted in Table 1, entries 1−5, comparable values for $M_{n,calcd}$ are found for the disperse blocks and the related discrete versions. Yet, MALDI-TOF analysis revealed the stark contrast for both the *o*DMS and *o*LA blocks when comparing the discrete and disperse samples, of which the latter contained at least 15 different oligomers (Figure S7B and C). Similar observations were made for the BCOs (entries 6−11, Figure 1 and Figure S7D and E). Here, purification of the final product by column chromatography led to a slightly larger variation in the *o*LA block length for the BCOs with a disperse *o*LA block obtained by ROP (entries 10 and 11). Still, all BCOs gave *o*LA volume fractions that were close to the desired fully symmetrical composition. Finally, dispersities of the BCOs ranged between $Đ < 1.00001$ for the discrete BCO and $Đ = 1.09$ for both BCOs with two disperse blocks, placing this set out of the dispersity range of previously studied BCOs.[12−14] Intermediate values for $Đ$ were found for the BCOs comprised of one discrete and one disperse block.

The thermal behavior of the BCOs was studied with differential scanning calorimetry (DSC). As shown in Figure S9, and summarized in Table 1, entries 6−11, and Table S1, this afforded the temperatures of the order−disorder transitions (ODTs), represented by endo- and exothermal transitions in the heating and cooling curves, respectively.[19,26] Interestingly, the ODT of nearly each BCO could be visualized by DSC, regardless of the presence of dispersity in either of the blocks. Only for BCO [$\mathbf{Si_{\sim 15}}$-$\mathbf{LA_{\sim 17}}$]-**PC**, no ODT was observed by DSC. For the other BCOs, the sharpness and position of the peaks varied significantly. Both [$\mathbf{Si_{15}}$-$\mathbf{LA_{17}}$] and [$\mathbf{Si_{\sim 15}}$-$\mathbf{LA_{17}}$], with discrete *o*LA blocks, gave narrow ODT signatures. In contrast, dispersity in the lactic acid block ([$\mathbf{Si_{15}}$-$\mathbf{LA_{\sim 17}}$]-**PC**, [$\mathbf{Si_{15}}$-$\mathbf{LA_{\sim 17}}$]-**ROP**, and [$\mathbf{Si_{\sim 15}}$-$\mathbf{LA_{17}}$]-**ROP**) resulted in signifi-

Scheme 1. Final Ligation Step in the Formation of Discrete and Disperse BCOs[a]

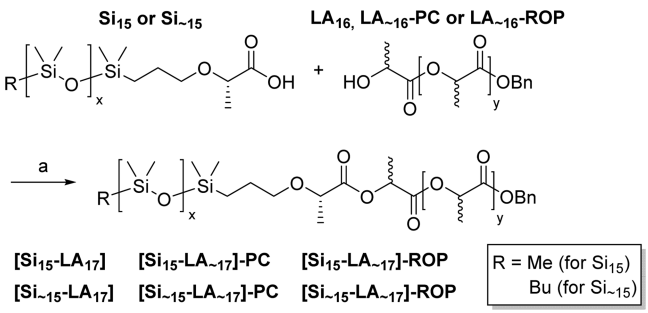

[a]Reagents and conditions: (a) EDC·HCl, DPTS, DCM, RT, O/N (58−82%).

DOI: 10.1021/acsmacrolett.7b00266
ACS Macro Lett. 2017, 6, 674−678

Table 1. Molecular Characterization Data for the Block Co-Oligomers and Separate Blocks

entry	compound[a]	#Si[b]	#LA[c]	$M_{n,calcd}$[d] [Da]	$M_{n,SEC}$ [Da]	$Đ$	N[e]	f_{LA}[f]	T_{ODT}[g] [°C]	d^*[h] [nm]
1	**Si_{15}**	15	-	1242	n.d.	<1.00001[j]	17.7	-	-	-
2	**$Si_{\sim 15}$**	15.2[i]	-	1299[i]	1360	1.15	18.7[i]	-	-	-
3	**LA_{16}**	-	16	1261	n.d.	<1.00001[j]	12.7	-	-	-
4	**$LA_{\sim 16}$-PC**	-	16.0[i]	1261[i]	1787	1.24	12.7[i]	-	-	-
5	**$LA_{\sim 16}$-ROP**	-	17.9[i]	1398[i]	2265	1.23	14.2[i]	-	-	-
6	[**Si_{15}-LA_{17}**]	15	17	2486	3852	<1.00001[j]	32.6	0.48	72.9	7.10
7	[**$Si_{\sim 15}$-LA_{17}**]	15.2[i]	17	2543[i]	4118	1.05	32.8[i]	0.47[i]	77.1	7.34
8	[**Si_{15}-$LA_{\sim 17}$**]-PC	15	16.2[i]	2429[i]	4015	1.08	30.5[i]	0.44[i]	82.9	7.20
9	[**$Si_{\sim 15}$-$LA_{\sim 17}$**]-PC	15.0[i]	16.7[i]	2464[i]	3999	1.09	30.9[i]	0.45[i]	-	7.45
10	[**Si_{15}-$LA_{\sim 17}$**]-ROP	15	21.0[i]	2774[i]	4964	1.07	36.1[i]	0.52[i]	79.5	7.72
11	[**$Si_{\sim 15}$-$LA_{\sim 17}$**]-ROP	15.0[i]	19.4[i]	2701[i]	4547	1.09	34.7[i]	0.51[i]	83.0	-

[a]Disperse blocks are indicated with a tilde (∼) character preceding the (desired) average block lengths. [b]Number of siloxane repeat units. [c]Number of lactic acid repeat units. [d]Calculated molecular weight, based on the number of Si and LA repeat units. [e]Number of segments based on a 110 Å^3 reference volume. [f]Lactic acid volume fraction, calculated using bulk densities for PDMS and PLA (0.95 and 1.24 g mL^{-1}, respectively).[19] [g]The reported values are for the heating run. [h]Domain spacing attributed to lamellar ordering. [i]Average value. [j]Calculated from relative peak intensities in the MALDI-TOF spectra.

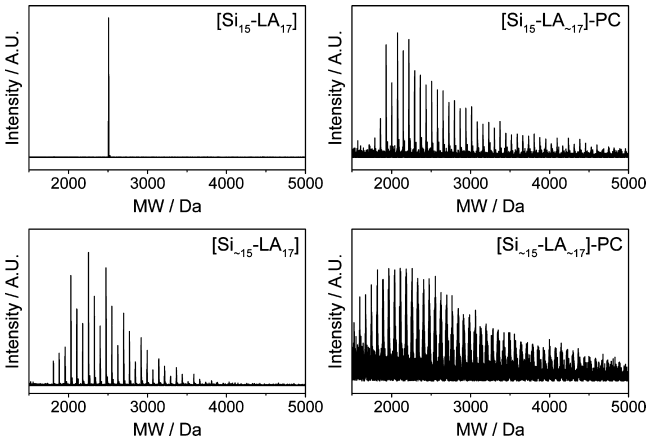

Figure 1. MALDI-TOF MS spectra (DCTB matrix) for *o*DMS−*o*LA BCOs.

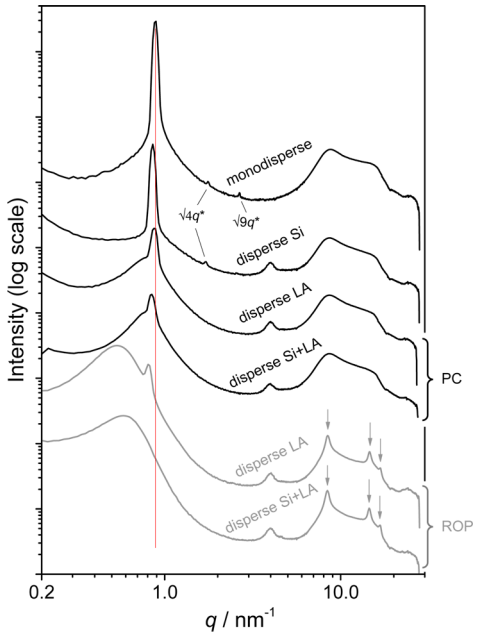

Figure 2. Room-temperature SAXS data for monodisperse and (partially) disperse BCOs. The data are shifted vertically for clarity. Higher-order Bragg reflections are indicated if present. The peak at q = 4 nm^{-1} results from background scattering (kapton tape). The vertical red line at q = 0.885 nm^{-1} is there to guide the eye.

cantly broader order−disorder transitions. Although not fully understood, this probably is partially related to the somewhat higher dispersity of the *o*LA block with respect to the *o*DMS block. In addition, a strong correlation between T_{ODT} and the dispersity was observed: T_{ODT} increased from T_{ODT} = 72.9 °C for the monodisperse [**Si_{15}-LA_{17}**] up to T_{ODT} = 83.0 °C for BCO [**$Si_{\sim 15}$-$LA_{\sim 17}$**]-**ROP** that has the highest dispersity ($Đ$ = 1.09). This suggests that the materials with higher dispersity are stable for lower values of χN ($\chi \propto T^{-1}$) and hence can be considered to have a more stable microphase-segregated state, exactly as described by the theoretical and experimental work.[12,27] Noteworthy here is the assumption that kinetic effects do not play a dominant role in the determination of T_{ODT} with DSC. The justifiability of this assumption follows from the small hysteresis between the transitions of each BCO in the heating and cooling run, as well as the negligible shift of T_{ODT} of, for example, [**Si_{15}-LA_{17}**] or [**$Si_{\sim 15}$-LA_{17}**] when the DSC measurement was repeated at 5 and 20 times slower heating and cooling rates (i.e., 2 °C min^{-1} and 0.5 °C min^{-1}, respectively).

Next, the extent of microphase separation in the BCOs was studied with small-angle X-ray scattering (SAXS) at room temperature. Azimuthal integration of the 2-D transmission scattering data resulted in 1-D patterns depicted in Figure 2. When focusing on the q-range 0.1−4 nm^{-1}, which corresponds to a size domain of approximately 1.6−60 nm, both [**Si_{15}-LA_{17}**] and [**$Si_{\sim 15}$-LA_{17}**] revealed a sharp principal scattering peak at q^* = 0.885 nm^{-1} and q^* = 0.856 nm^{-1}, respectively. This corresponds to domain spacings ($d^* = 2\pi/q^*$) of d^* = 7.10 nm for [**Si_{15}-LA_{17}**] and d^* = 7.34 nm for [**$Si_{\sim 15}$-LA_{17}**]. Additional reflections at q-values $\sqrt{4}q^*$ (both BCOs) and $\sqrt{9}q^*$ (discrete BCO only) confirmed the lamellar ordering of the samples. Increasing the dispersity in the *o*DMS block has a negative—albeit small—effect on the quality of microphase separation. Besides, a small but significant decrease in q^* (i.e., an increase of the domain spacing) was seen after introduction of dispersity in the siloxane block. This is in line with SCFT predictions and previous experimental work[13] but never observed for materials with such low dispersities. In sharp contrast, the scattering curves of BCOs with a disperse *o*LA block lack any higher-order reflections and are largely dominated by a broad reflection that

DOI: 10.1021/acsmacrolett.7b00266
ACS Macro Lett. 2017, 6, 674−678

is typical for a disordered BCP.[1,28] This reflection nearly overshadows the aforementioned primary peak that belongs to the microphase-segregated state and is the only observable reflection at low q for BCO [**Si$_{\sim15}$-LA$_{\sim17}$**]-**ROP**. It is currently unclear why [**Si$_{\sim15}$-LA$_{\sim17}$**]-**ROP** is seemingly disordered according to SAXS but still gives a weak thermal signature in the DSC traces. Overall, the scattering data reveal that all of the BCOs with a disperse *o*LA block primarily reside in a disordered state, although partially (lamellar) ordered domains coexist in most samples. Apparently, increasing dispersity in either the *o*DMS or *o*LA block affects the lamellar organization to a different extent. The origin hereof is not entirely understood but is likely related to the disparate molecular makeup of the blocks, different block length distributions, or differences in statistical segment lengths.

Additionally, we performed variable-temperature (VT) SAXS measurements with BCO [**Si$_{15}$-LA$_{17}$**] (Figure S10). Here, a drastic decrease in the intensity of the primary scattering peak was found between 72 and 74 °C. This reduction in scattering intensity is related to the formation of a disordered state,[29] and the temperature of this transition confirms the T_{ODT} value that was found with DSC.

Initially, we were intrigued by the higher level of disordered regions in the set of BCOs with a disperse *o*LA block obtained via ROP compared to those obtained by polycondensation. First, the dispersities of [**Si$_{15}$-LA$_{\sim17}$**]-**PC** and [**Si$_{15}$-LA$_{\sim17}$**]-**ROP** are nearly equal, as are the dispersities of [**Si$_{\sim15}$-LA$_{\sim17}$**]-**PC** and [**Si$_{\sim15}$-LA$_{\sim17}$**]-**ROP**. Besides, N is slightly higher for both BCOs produced with ROP than the PC analogues, which principally should lead to a more facile formation of an *ordered* structure. However, additional scattering experiments in the q-range 4−30 nm^{-1} (size domain of approximately 2−16 Å) revealed a clear contrast between the materials obtained by PC or ROP. As expected, two partially resolved, broad peaks at q = 8.6 nm^{-1} and q = 14.8 nm^{-1} were found in the scattering data of the BCOs for which polycondensation was employed. These reflections represent the siloxane and oligolactic acid halos of the two amorphous constituents of the BCO, respectively, and are identical to the halos that were observed for [**Si$_{15}$-LA$_{17}$**] and [**Si$_{\sim15}$-LA$_{17}$**] (i.e., BCOs with a discrete *o*LA block). Contrarily, three additional, sharper peaks appeared in the scattering profiles of the BCO with disperse *o*LA blocks obtained by ROP (marked with arrows in Figure 2). The location of these peaks is in exact correspondence with those found for the stereocomplex of isotactic, crystalline PLA,[30] which is suggestive of a higher degree of isotacticity in the disperse *o*LA blocks. Indeed, ^{13}C NMR experiments provided qualitative evidence for an above-average amount of isotactic tetrads and hexads in the BCOs with a disperse *o*LA block obtained via ROP as opposed to those with the discrete block or disperse block made by polycondensation (more details in the Supporting Information, Figure S11).[31,32] Clearly, the higher degree of isotacticity amplifies the adverse effect of dispersity in the *o*LA block on the formation of an ordered structure. More generally, we would like to emphasize that, in low MW polymers, the effect of intermolecular interactions resulting from the end groups and interblock connectivities might no longer be neglected. In fact, a publication by the Hawker research group, accompanying this work, describes a set of BCOs with comparable length and dispersities but incorporating different chemical structures.[25] Here, they reveal an exactly opposite trend of T_{ODT} versus dispersity yet a very similar effect on the domain spacings. However, we would like to stress that these apparent differences should not be conceived purely as contradictory behavior but merely highlight that the (phase) behavior of high χ−low N block copolymers still is highly unpredictable. Primarily, the combined results show that the field is starting to unfold its secrets in the structure−property relationships of high χ−low N materials.

In conclusion, we demonstrated that the phase behavior of a high χ−low N BCO is very sensitive to the introduction of minor amounts of dispersity. An increase of dispersity resulted in widening of the domain spacing. Furthermore, two important terms that quantify and qualify phase behavior—and are often erroneously used interchangeably—show two pronounced, yet exactly opposite, trends. Upon switching from a discrete to a considerably less "monodisperse" BCO, there is (1) an increase of the *stability* of the microphase-segregated state, expressed as an increase of the T_{ODT}, accompanied by (2) a decrease of the overall *degree of ordering* in the samples. Finally, our samples illustrated that variations in local stereoregularity have a strong influence on BCO phase behavior. In view of the forth-going trend toward materials that are becoming too exclusive to be classified as either polymers or small molecules (e.g., thermotropic liquid crystals), we will continue our explorative work on discrete polymeric materials.

■ ASSOCIATED CONTENT

Supporting Information

The Supporting Information is available free of charge on the ACS Publications website at DOI: 10.1021/acsmacrolett.7b00266.

Experimental procedures, characterization data for all compounds, Table S1, and Figures S1−S11 (PDF)

■ AUTHOR INFORMATION

Corresponding Authors

*E-mail: e.w.meijer@tue.nl.

*E-mail: a.palmans@tue.nl.

Notes

The authors declare no competing financial interest.

■ ACKNOWLEDGMENTS

We gratefully thank the Hawker research group for the constructive discussion and sharing of relevant research data. This work is financed by the Royal Netherlands Academy of Arts and Sciences and the Dutch Ministry of Education, Culture, and Science (Gravity program 024.001.035).

■ REFERENCES

(1) Leibler, L. *Macromolecules* **1980**, *13*, 1602−1617.

(2) Sinturel, C.; Bates, F. S.; Hillmyer, M. A. *ACS Macro Lett.* **2015**, *4*, 1044−1050.

(3) Jung, Y. S.; Chang, J. B.; Verploegen, E.; Berggren, K. K.; Ross, C. A. *Nano Lett.* **2010**, *10*, 1000−1005.

(4) Cushen, J. D.; Bates, C. M.; Rausch, E. L.; Dean, L. M.; Zhou, S. X.; Willson, C. G.; Ellison, C. J. *Macromolecules* **2012**, *45*, 8722−8728.

(5) Cushen, J. D.; Otsuka, I.; Bates, C. M.; Halila, S.; Fort, S.; Rochas, C.; Easley, J. A.; Rausch, E. L.; Thio, A.; Borsali, R.; Willson, C. G.; Ellison, C. J. *ACS Nano* **2012**, *6*, 3424−3433.

(6) Pitet, L. M.; Wuister, S. F.; Peeters, E.; Kramer, E. J.; Hawker, C. J.; Meijer, E. W. *Macromolecules* **2013**, *46*, 8289−8295.

(7) Luo, Y.; Montarnal, D.; Kim, S.; Shi, W.; Barteau, K. P.; Pester, C. W.; Hustad, P. D.; Christianson, M. D.; Fredrickson, G. H.; Kramer, E. J.; Hawker, C. J. *Macromolecules* **2015**, *48*, 3422−3430.

DOI: 10.1021/acsmacrolett.7b00266
ACS Macro Lett. 2017, 6, 674−678

(8) Durand, W. J.; Blachut, G.; Maher, M. J.; Sirard, S.; Tein, S.; Carlson, M. C.; Asano, Y.; Zhou, S. X.; Lane, A. P.; Bates, C. M.; Ellison, C. J.; Willson, C. G. *J. Polym. Sci., Part A: Polym. Chem.* **2015**, *53*, 344−352.
(9) Lynd, N. A.; Meuler, A. J.; Hillmyer, M. A. *Prog. Polym. Sci.* **2008**, *33*, 875−893.
(10) Beardsley, T. M.; Matsen, M. W. *Eur. Phys. J. E: Soft Matter Biol. Phys.* **2008**, *27*, 323−333.
(11) Beardsley, T. M.; Matsen, M. W. *Macromolecules* **2011**, *44*, 6209−6219.
(12) Lynd, N. A.; Hillmyer, M. A. *Macromolecules* **2007**, *40*, 8050−8055.
(13) Lynd, N. A.; Hillmyer, M. A. *Macromolecules* **2005**, *38*, 8803−8810.
(14) Lynd, N. A.; Hamilton, B. D.; Hillmyer, M. A. *J. Polym. Sci., Part B: Polym. Phys.* **2007**, *45*, 3386−3393.
(15) Park, S.; Kwon, K.; Cho, D.; Lee, B.; Ree, M.; Chang, T. *Macromolecules* **2003**, *36*, 4662−4666.
(16) Park, S.; Cho, D.; Ryu, J.; Kwon, K.; Lee, W.; Chang, T. *Macromolecules* **2002**, *35*, 5974−5979.
(17) Park, S.; Ryu, D. Y.; Kim, J. K.; Ree, M.; Chang, T. *Polymer* **2008**, *49*, 2170−2175.
(18) Bates, C. M.; Bates, F. S. *Macromolecules* **2017**, *50*, 3−22.
(19) Van Genabeek, B.; De Waal, B. F. M.; Gosens, M. M. J.; Pitet, L. M.; Palmans, A. R. A.; Meijer, E. W. *J. Am. Chem. Soc.* **2016**, *138*, 4210−4218.
(20) Widin, J. M.; Schmitt, A. K.; Schmitt, A. L.; Im, K.; Mahanthappa, M. K. *J. Am. Chem. Soc.* **2012**, *134*, 3834−3844.
(21) Schmitt, A. L.; Mahanthappa, M. K. *Soft Matter* **2012**, *8*, 2294.
(22) Widin, J. M.; Kim, M.; Schmitt, A. K.; Han, E.; Gopalan, P.; Mahanthappa, M. K. *Macromolecules* **2013**, *46*, 4472−4480.
(23) Matsushita, Y.; Noro, A.; Iinuma, M.; Suzuki, J.; Ohtani, H.; Takano, A. *Macromolecules* **2003**, *36*, 8074−8077.
(24) Noro, A.; Cho, D.; Takano, A.; Matsushita, Y. *Macromolecules* **2005**, *38*, 4371−4376.
(25) Oschmann, B.; Lawrence, J.; Schulze, M. W.; Ren, J. M.; Anastasaki, A.; Luo, Y.; Nothling, M. D.; Pester, C. W.; Delaney, K. T.; Connal, L. A.; McGrath, A. J.; Clark, P. G.; Bates, C. M.; Hawker, C. J. *ACS Macro Letters* **2017**, DOI: 10.1021/acsmacrolett.7b00262.
(26) Lee, S.; Gillard, T. M.; Bates, F. S. *AIChE J.* **2013**, *59*, 3502−3513.
(27) Pandav, G.; Ganesan, V. *J. Chem. Phys.* **2013**, *139*, 214905.
(28) Bates, F. S. *Macromolecules* **1985**, *18*, 525−528.
(29) Sakamoto, N.; Hashimoto, T. *Macromolecules* **1995**, *28*, 6825−6834.
(30) Tsuji, H. *Macromol. Biosci.* **2005**, *5*, 569−597.
(31) Kasperczyk, J. E. *Macromolecules* **1995**, *28*, 3937−3939.
(32) Zhao, P.; Qin-Feng, W.; Zhong, Q.; Nai-Wen, Z.; Ren, J. *J. Appl. Polym. Sci.* **2010**, *115*, 2955−2961.

DOI: 10.1021/acsmacrolett.7b00266
ACS Macro Lett. 2017, 6, 674−678